Available online at www.sciencedirect.com
SCIENCE DIRECT®
Journal of Solid State Chemistry 172 (2003) 451–457
JOURNAL OF SOLID STATE CHEMISTRY
http://elsevier.com/locate/jssc

Synthesis, structure and magnetic properties of the $S = 1/2$, one-dimensional antiferromagnet, $Y_5Re_2O_{12}$

Lisheng Chi, J.F. Britten, and J.E. Greedan*

Department of Chemistry & Brockhouse Institute for Materials Research, McMaster University, 1280 Main Street West, Hamilton, Ont., Canada L8S 4M1

Received 27 August 2002; accepted 14 December 2002

Abstract

Single crystals of $Y_5Re_2O_{12}$ have been grown, and the crystal structure has been determined by X-ray diffraction. This compound crystallizes in space group $C2/m$ with cell dimensions of $a = 12.4081(10)$ Å $b = 5.6604(5)$ Å, $c = 7.4951(6)$ Å, $\beta = 107.837(3)^\circ$, $Z = 2$. The final refinement led to $R1 = 0.0238$, $WR2 = 0.0459$ for 1053 observed reflections with $F > 4\sigma(F_0)$. Edge-sharing ReO_6 octahedra form infinite linear $[ReO_2O_{4/2}]_n$ chains along the b direction with alternating short and long Re–Re distances. Three crystallographically independent yttrium atoms surround O2 to form OY_4 tetrahedra, which share edges and corners in the ab plane to form a two-dimensional Y_5O_4 network which separates the $[ReO_2O_{4/2}]_n$ magnetic chains. This compound is therefore isostructural with the series $Ln_5Re_2O_{12}$ Ln = Gd–Lu, which have been known since 1969. The average Re oxidation state is +4.5 in the chains and a reasonable, if qualitative MO scheme results in one unpaired electron per Re dimer. Consistent with this, magnetic susceptibility data can be fitted to the one-dimensional antiferromagnetic Heisenberg model with $S = 1/2$ and parameters $J^{intra}/k = -89(1)K$, $g = 2.15(4)$ and $\chi(TIP) = 5(1) \times 10^{-4}$ emu/mol. There is no sign of long-range magnetic order down to 2 K. These results are contrasted with those for the isostructural $Y_5Mo_2O_{12}$.

Keywords: Re^{4+}/Re^{5+} mixed valent oxides; $[ReO_2O_{4/2}]_n$ chains; Y_5O_4 layers; $S = 1/2$ linear change antiferromagnet

1. Introduction

Low-dimensional solids possess a high anisotropy in the spatial distribution of chemical bonds which results in a large anisotropy in a certain physical properties. In such systems either exact or very accurate numerical models for physical properties, especially magnetism, exist and thus in recent years, low-dimensional materials have been of great interest to physicists and chemists. A variety of novel physical phenomena have been found in low-dimensional inorganic transition metal oxides, such as the spin-Peierls instability for $GeCuO_3$[1] charge-density-wave in quasi-one-dimensional $K_{0.3}MoO_3$ [2], high-T_c cuprates with quasi-two-dimensional structural and electronic properties [3], and spinon–holon separation for $SrCuO_2$ [4]. These phenomena reflect the rich and complex nature of the correlated electrons in these systems, most of which are based on transition elements of the 3*d* series.

Oxides of the 4*d* and 5*d* elements also exhibit low-dimensional structural features. Among these are the fluorite-related compounds La_3MO_7 where M = Ru, Os or Mo which show one-dimensional magnetic correlations due to linear chains of corner-sharing MO_5 octahedra [5,6]. Other possibilities are Re-based oxides, $Ln_5Re_2O_{12}$, Ln = Gd–Lu,Y, which have been known since 1969 [7–11]. In these materials Re–O octahedral units are connected by sharing common *trans* edges to form infinite $[ReO_2O_{4/2}]_n$ chains which are separated by rare-earth atoms. The intrachain Re–Re distances alternate between short and long suggesting the formation of Re_2O_{10} dimers. As the Re oxidation state is +4.5 there will be one unpaired electron per Re_2 dimer. In the two materials for which magnetic studies exist to date, the large magnetic moments of Tb and Ho mask the magnetism due to the Re chains and the data are available over a limited temperature range [7]. In this work a compound containing a non-magnetic

*Corresponding author. Fax: 905-522-2773.
E-mail address: greedan@mcmail.cis.mcmaster.ca (J.E. Greedan).

0022-4596/03/$ - see front matter © 2003 Elsevier Science (USA). All rights reserved.
doi:10.1016/S0022-4596(03)00033-1

rare-earth, $Y_5Re_2O_{12}$, was studied to investigate the magnetic properties of the Re chains. Here, the synthesis, crystal structure, and magnetic properties of $Y_5Re_2O_{12}$ are reported.

2. Experimental

2.1. Synthesis

The single crystals of $Y_5Re_2O_{12}$ were obtained, serendipitiously, from an attempt to synthesize $Y_5Re_3MnO_{16}$. Y_2O_3 (Reaction, 99.9%), ReO_3 (Rhenium alloys), Re (Rhenium alloys) and MnO (Alfa Aesar, 99.5%) were mixed with the ratio 5:5:1:2, ground, pressed into a pellet which was loaded in a Pt crucible and sealed in an evacuated silica tube that was kept at 1050°C for 2 days, then cooled to room temperature at the rate of 12°C/m. Many black, needle-shaped crystals of $Y_5Re_2O_{12}$ formed on the surface of the pellet.

A powder sample of $Y_5Re_2O_{12}$ was prepared from Y_2O_3, ReO_3 and Re according to the reaction:

$$5Y_2O_3+5ReO_3+Re \rightarrow 2Y_5Re_2O_{12}.$$

A 1 g sample was prepared from stoichiometric quantities of Y_2O_3, ReO_3 and Re which were weighed, mixed, ground, pressed into pellets and sealed in an evacuated silica tube, which was heated in a muffle furnace at 1050°C for several days with intermittent grinding. The black product was checked for phase purity by Guinier–Hagg camera X-ray data.

2.2. Structure determination

A needle-shaped crystal with approximate dimensions of $0.02 \times 0.03 \times 0.5$ mm was chosen for data collection, which was carried out at room temperature on a Bruker P4 CCD diffractometer with the aid of rotating anode graphite-monochromated Mo$K\alpha$ radiation. A least-squares refinement of the settings of 944 centered reflections in the range of $6.8° < 2\theta < 71.7°$ were consistent with a centered monoclinic cell with the dimensions of $a = 12.4081(10)$ Å, $b = 5.6604(5)$ Å, $c = 7.4951(6)$ Å and $\beta = 107.837(3)°$.

Diffraction data were collected with ϕ and ω scans in the range of $5.7° < 2\theta < 72.6°$. The program SAINT [12] was used for data reduction, including integration and Lorentz and polarization corrections. The program SADABS [13] was used for empirical absorption corrections. The systematic absences ($h + k = 2n + l$ for $h\,k\,l$) for 6150 reflections and good agreement among the Friedel pairs suggested the centrosymmetric monoclinic space group $C2/m$. The successful structure refinement confirmed this assignment.

The structure solution and refinement of the title compound were performed with the SHELXTL 5.03 software package [14,15]. Direct methods were applied to reveal four heavy atom positions, one of which was assigned to Re and three to Y atoms. A subsequent difference Fourier synthesis revealed four other independent peaks, which were easily assigned to O atoms on basis of the distances from peaks to Re and Y atoms. The refinement of all positions with isotropic thermal parameters led to $R1 = 3.35\%$. The anisotropic refinement converged at $R1 = 3.17\%$. Nonetheless, several rather large residual peaks were present in the difference map in the Re1, Y3 layer at approximately $x = 0$. At this stage the possibilities of both twinning and partial disorder were considered. While twinning had been observed in crystals of other members of the series [7,10,11], examination of the data showed no evidence of C-centering violations in this case. A partial disorder mechanism [11] proved more successful. A shift of $(0, 0, 0.5)$ in the Re1, Y3, O3, O4 layer with an occupancy of 2.27(8)% accounted for the observed density. The final refinement led to $R1 = 2.38\%$ for 1053 reflections with $F > 4\sigma(F_0)$, $wR2 = 4.59\%$, and $S = 1.081$. The U11 of O3 (~ 0.014) is remarkably higher than U22 (~ 0.005) and U33 (~ 0.004), indicating that O3 prefers displacement along the a direction. The highest residual peak and the deepest hole are 2.10 e/Å^3 (2.01 Å from Y2) and −3.05 e/Å^3 (0.71 Å from Re1). Details on the structure refinement parameters are reported in Table 1. The final atomic coordinates and selected bond distances are listed in Tables 2 and 3, respectively. Further details of the crystal structure investigation can be obtained from the Fachinfromationszentrum Karlsruhe, 76344 Eggenstein-Leopoldshafen, Germany (fax: (49) 7247-808-666; e-mail: crysdata@fiz.karlsruhe.de) on quoting the depository number CSD-412720.

2.3. Magnetic susceptibility measurement

Magnetic susceptibility measurements were performed on a powder sample in a gelatin capsule container using a Quantum Design MPMS SQUID magnetometer in a temperature range from 5 to 350 K with an applied field of 1000 Oe. The data were corrected for diamagnetic core contributions of -2.6×10^{-4} emu/mol.

3. Results and discussion

3.1. Crystal structure

The crystal structure of $Y_5Re_2O_{12}$ is isotypic with $Ho_5Re_2O_{12}$ [7] except for slightly disordered Re1, Y3, O3 and O4 atoms. Although the space group of $Dy_5Re_2O_{12}$ [10,11] was determined to be $P2_1/m$ from a twinned crystal, this was later assigned as $B2/m$ from

a twinned crystal of $Ho_5Re_2O_{12}$. Here the structure is described in the standard setting, $C2/m$.

Fig. 1 presents the crystal structure of $Y_5Re_2O_{12}$. The dominant structure feature consists of one-dimensional chains of edge-shared magnetic Re octahedra, which are separated by non-magnetic Y and O atoms. As shown in Fig. 2, the rhenium atom is coordinated by six oxygen atoms with irregular octahedral geometry. Re–O distances range between 1.946(3) and 2.079(3) Å with an average value of 1.998 Å. Within the chain, two ReO_6 octahedra are connected by sharing an O_3–O_3 edge and with an Re–Re bond of 2.4466(5) Å to form dimeric Re_2O_{10} units, which are connected to other such dimers by sharing O4–O4 edges with the resultant Re–Re separation of 3.2138(5) Å. The Re–Re–Re intrachain angle is 180.0°. Thus, these octahedra form infinite linear chains of composition $[ReO_2O_{4/2}]_n$ through sharing common edges with alternating short and long Re–Re distances. The rhenium atoms in $Y_5Re_2O_{12}$ have an average oxidation state of +4.5. The shorter Re–Re distance is comparable to those in $La_4Re_6O_{19}$ (Re–Re: 2.42 Å) [16] with Re oxidation state +4.33, $Ho_5Re_2O_{12}$ (Re–Re: 2.436 Å) [17] with Re oxidation state +4.5 and $Nd_4Re_2O_{11}$ (Re–Re: 2.42 Å) [18] with Re oxidation state +5.0. It has been noted that the relationship between bond length and nominal bond order in multiple bonded Re dimers in oxides is decidedly non-linear [19]. A bond valence calculation, carried out using the program VaList, [20] shows that the calculated oxidation states for Re1, Y1, Y2 and Y3 are 4.18, 3.01, 2.91, 3.05, respectively, and are in good agreement with the formal oxidation states of +4.5 and +3, respectively, within 10% error. The calculated valences for O1, O2, O3 and O4 are 1.88, 1.93, 2.7 and 1.93, respectively. The unusually large valence for O3 might indicate π-bonding interactions between O3 and Re, because O3 adopts a distorted trigonal–planar coordination with sp^2

Table 1
Crystal data of $Y_5Re_2O_{12}$

Chemical formula	$Y_5Re_2O_{12}$
*F*w	1008.95
Crystal size (mm^3)	$0.02 \times 0.03 \times 0.5$
Crystal shape	Needle
Crystal system	Monoclinic
Space group	$C2/m$
Lattice constants	$a = 12.4081(10)$ Å $b = 5.6604(5)$ Å $c = 7.4951(6)$ Å $\beta = 107.837(3)°$
Cell volume ($Å^3$)	501.11(7)
Z	2
ρ_{calc} (g/cm^3)	6.687
F (000)	882
μ (mm^{-1})	52.72
Scan mode	ϕ, ω
Radiation wavelength (Å)	0.71073
Range of data collection	$5.7° < 2\theta < 72.6°$
Range of *h k l*	$-19 < h < 20$, $-9 < k < 7$, $-11 < l < 12$
Total measured reflections	6150
Unique reflections	1204
Observed reflections ($I > 2\sigma(I_0)$)	1053
Extinction coefficient	0.0018(1)
Variable parameters	59
*R*1	0.0238
w*R*2	0.0490
S (Goodness-of-fit)	1.086
The highest and lowest residues ($e/Å^3$)	2.10, −3.05

$R1 = \sum|F_o| - |F_c|/\sum|F_o|$.
$wR2 = 1/[s^2(F_o^2) + (0.0216P)^2 + 3.80P]$ where $P = (F_o^2 + 2F_c^2)/3$.

Table 3
Selected bond distances (Å) for $Y_5Re_2O_{12}$

Re1–O2	1.946(3) × 2	Y2–O2	2.428(3) × 2
Re1–O3	1.969(4) × 2	Y1–O2	2.279(3) × 2
Re1–O4	2.079(3) × 2	Y1–O1	2.292(3) × 2
Re1–Re1	2.4466(5)	Y1–O4	2.317(4)
Re1–Re1	3.2138(5)	Y1–O2	2.458(3) × 2
Y2–O1	2.281(3) × 2	Y3–O3	2.205(5) × 2
Y2–O1	2.322(3) × 2	Y3–O1	2.305(3) × 4
Y2–O4	2.381(5)		

Table 2
Atomic coordinates and displacement parameters for $Y_5Re_2O_{12}$

Atom	*x*	*y*	*z*	Occupancy (%)	U_{eq} ($Å^2$)
Re1	0	0.21612(4)	0	97.73(8)	0.00308(7)
Y1	0.31373(5)	0	0.17336(8)	100	0.00544(11)
Y2	0.30447(5)	0	0.64140(8)	100	0.00482(11)
Y3	0	0	0.5	97.73(8)	0.00495(15)
O1	0.3464(3)	0.2489(5)	0.4255(4)	100	0.0055(5)
O2	0.1638(3)	0.2528(5)	0.0825(4)	100	0.0060(5)
O3	0.0006(4)	0	0.7945(7)	97.73(8)	0.0069(8)
O4	0.0010(4)	0.5	0.1766(6)	97.73(8)	0.0049(8)
Re1*A*	0	0.208(1)	0.5	2.27	0.00308
Y3*A*	0	0	0	2.27	0.00495
O3*A*	−0.01(2)	0	0.29(3)	2.27	0.0069
O4*A*	0.01(2)	0.5	0.70(3)	2.27	0.0049

All atoms were refined anisotropically. The minor components were given the temperature factors of their counterparts. $U_{eq} = 1/3\Sigma_i\Sigma_j(U^{ij}a_ia_j\mathbf{a}_i.\mathbf{a}_j)$.

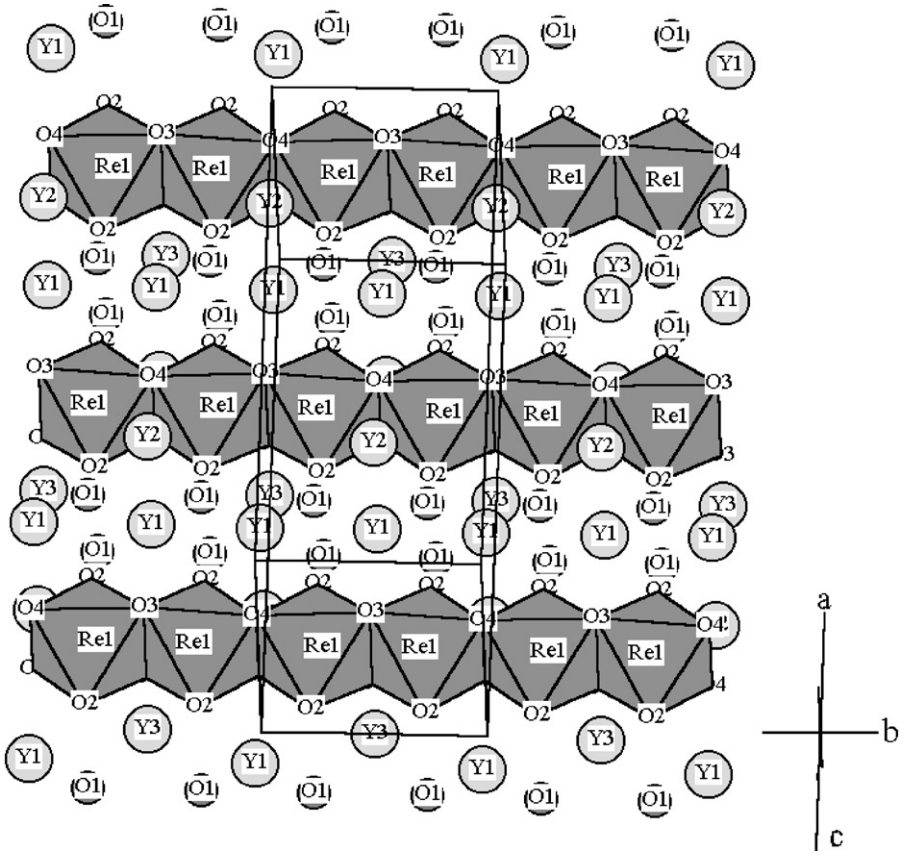

Fig. 1. The crystal structure of $Y_5Re_2O_{12}$ showing the infinite chains of edge sharing. $ReO_2O_{4/2}$ octahedra separated by yttrium and oxygen atoms.

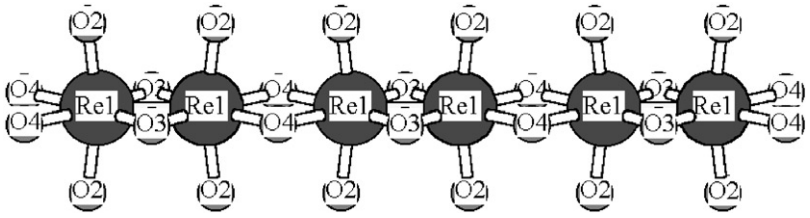

Fig. 2. A section of an infinite chain of $ReO_2O_{4/2}$ edge-sharing octahedra in $Y_5Re_2O_{12}$, along the *b* direction with alternating short (2.4467 Å) and long (3.2137 Å), Re–Re distances.

hybridization and can provide a lone *p* orbital to interact with rhenium in a π bonding mode.

There are three crystallographically independent yttrium atoms in $Y_5Re_2O_{12}$. Both Y1 and Y2 are coordinated by seven oxygen atoms with mono-capped trigonal prismatic geometry, shown in Fig. 3. The Y3 atom is octahedrally coordinated by six oxygen atoms. Y–O bond distances vary from 2.280(3) to 2.457(3) Å with a mean value 2.339 Å for Y1, 2.281(3)–2.428(3)Å with a mean value 2.349 Å for Y2, and 2.205(5)–2.305(3) Å with a mean value 2.272 Å for Y3. Thus, as expected, the average Y–O distances decrease with decreasing coordination number of the central Y atom. The O1, O2, O4 atoms are tetrahedrally coordinated while O3 shows trigonal–planar coordination. Two Y2, one Y1 and one Y3 atoms coordinate to O1 to form a distorted OY_4 tetrahedron which is connected to three other OY_4 tetrahedra by edge sharing and one OY_4 tetrahedron by corner sharing to form a double tetrahedral chain along the *b* direction. These chains are linked through the common corner O4 to construct a two-dimensional Y_5O_4 network on the *ab* plane (Fig. 4). Therefore, the structure of $Y_5Re_2O_{12}$ can also be described as consisting of infinite chains of sharing-edge ReO_6, separated by a two-dimensional Y_5O_4 tedrahedral framework as represented in Fig. 5.

The oxidation state +4.5 for rhenium indicates that 2.5 electrons on each Re atom (or 5 electrons per Re_2

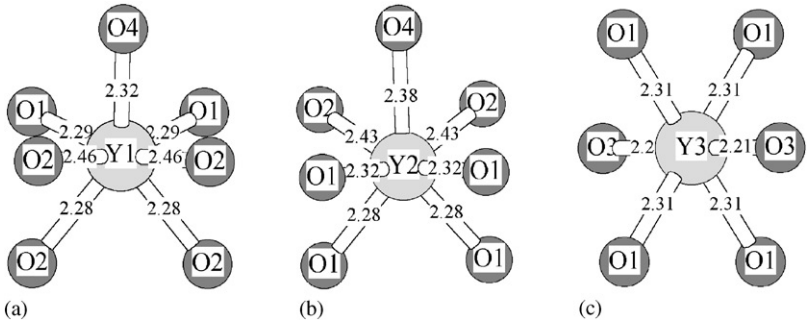

Fig. 3. Coordination environments of the yttrium atoms in $Y_5Re_2O_{12}$. (a) Y2, (b) Y1, and (c) Y3. The Y–O distances are indicated.

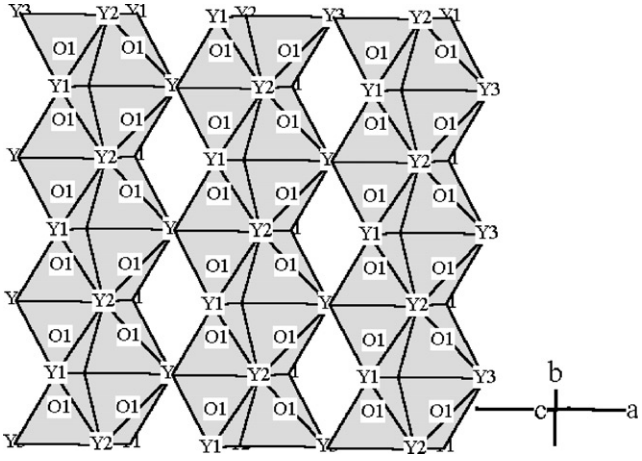

Fig. 4. The Y_5O_4 network formed by edge and corner sharing of OY_4 tetrahedra in the *ab* plane.

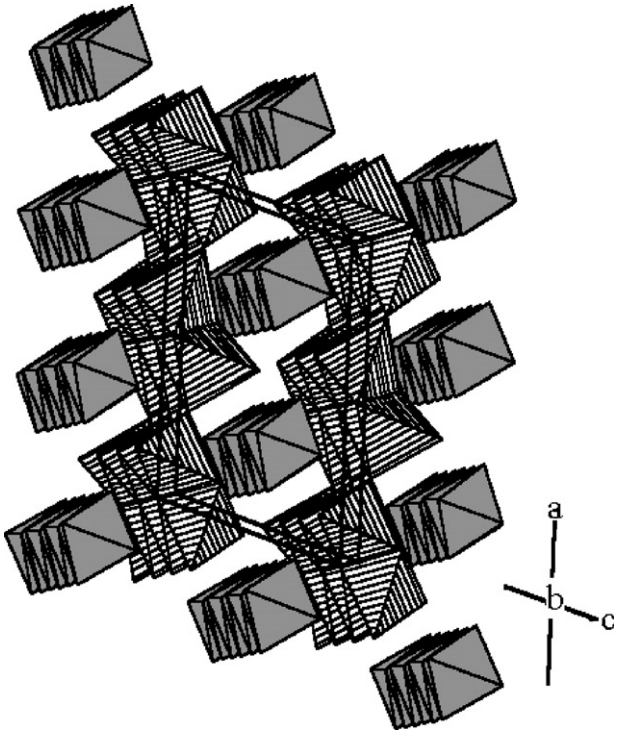

Fig. 5. A view of the crystal structure of Y_5ReO_{12} in full polyhedral representation showing the separation of the $ReO_2O_{4/2}$ chains by the Y_5O_4 layers.

group) are not involved in Re–O bonds. It is reasonable to assign four of these to bonding orbitals to form a Re = Re double bond with one σ bond and one π bond, [21] which leaves one electron in an orthogonal π orbital which may be bonding or non-bonding.

This unique electron is likely to be localized within the Re_2O_{10} unit. It is unlikely to be delocalized along the chain due to the long Re–Re interdimer distance of 3.2138 Å. For example, the Re–Re separation in the element is 2.75 Å. It has been conjectured that the structure of the Re chain in the related Ln_2ReO_5 phases and also, presumably in the $Ln_5Re_2O_{12}$ series, is a result of a Peierls distortion which sets in at a very high temperature [19]. So the unpaired electron should localize within the Re_2O_{10} unit and the compound should behave as a semiconductor with a local moment appropriate to $S = 1/2$ per formula unit. This can be confirmed by magnetic measurements.

The same structural type has been found in $Y_5Mo_2O_{12}$, [22] where infinite chains consist of edge-sharing MoO_6 octahedra with alternating short and long Mo–Mo distances and comparisons will be made.

3.2. Magnetic properties

Fig. 6 shows the magnetic susceptibility as a function of temperature within the range 5–350 K at an applied field of 1000 Oe. The most prominent features of the data are the presence of a broad, weak peak around with a maximum near $\sim$125 K and a sharply increasing susceptibility at the lowest temperatures. It is also important to mention that, although not shown in Fig. 6, there is no difference between the data obtained in the field-cooled (FC) and the zero-field-cooled (ZFC) mode. As the broad maximum is a characteristic of short-range magnetic correlations, an attempt was made to fit these data to an expression consisting of three

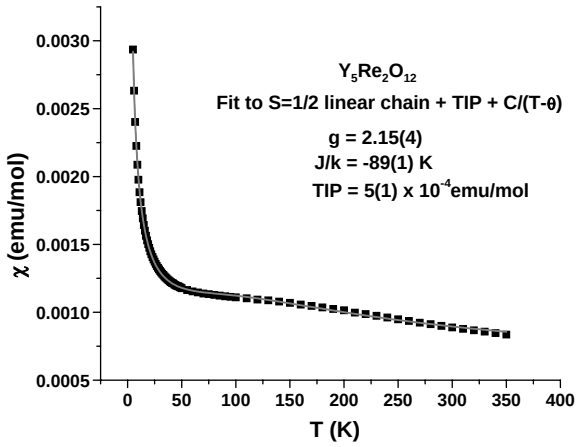

Fig. 6. The magnetic susceptibility of $Y_5Re_2O_{12}$. The solid squares are the data and the solid line is a fit to a function consisting of a one-dimensional $S = 1/2$ Heisenberg model plus a low-temperature Curie–Weiss term and a temperature-independent paramagnetic term. The fitting parameters are: $g = 2.15(1)$, $J^{intra}/k = -89(1)$ K, $C = 0.0122$ emu K/mol, $\theta = -0.99(6)$ K and $\chi(TIP) = 5.2(1) \times 10^{-4}$ emu/mol. See text for details.

terms as below

$$\chi(T) = \chi_{1D}(T) + \chi_P(T) + \chi_0, \quad (1)$$

where χ_{1D} represents a one-dimensional Heisenberg AF model after Bonner and Fisher and Weng [23,24], χ_P models the low-temperature paramagnetic tail using a Curie–Weiss expression and χ_0 is a temperature-independent contribution. The following equation [25] was used for the χ_{1D} term:

$$\chi(T) = \left(\frac{Ng^2\mu_B}{kT}\right)\frac{(0.25 + 0.18297x^2)}{(1 + 1.5467x + 3.4443x^3)}, \quad (2)$$

where $x = |J^{intra}|/k$, J^{intra} being the intrachain exchange constant, and N, μ_B, and k are Avogadro's constant, the Bohr magneton and Boltzmann's constant, respectively. The fit of the data of Fig. 6 to Eq. (2) by a least-squares method yielded $g = 2.15(4)$, $J/k = -89(1)$ K, $\chi_0 = 5.2(1) \times 10^{-4}$ emu/mol, $C = 1.22(1) \times 10^{-2}$ emu/mol, $\theta = -0.99(6)$ K. The effective g factor is slightly larger than might be expected but is not unreasonable. The intrachain exchange, J^{intra}, represents the coupling between the unpaired electrons localized within the dimers along the Re chains. Regarding the Curie–Weiss constants associated with the low-temperature data, the Curie constant is about 3% of the value expected for $S = 1/2$ electrons and the Weiss temperature is nearly zero. These features may arise from the observed crystallographic disorder which is of the same order of magnitude.

As mentioned earlier, an isostructural compound, $Y_5Mo_2O_{12}$, exists which has been characterized structurally and magnetically [22]. In this material, Mo also exhibits an average oxidation state of +4.5 which implies that three electrons are associated with each Mo_2 dimer and thus a bond order of 1.5. The published magnetic properties of this compound differ remarkably from those of the Re analog. First of all, nearly the entire temperature range from ~10 to 300 K can be fit to a Curie–Weiss law with an effective moment of 1.70 μ_B, the spin-only value for one unpaired electron, and a small Weiss temperature, $\theta = -7.5$ K. There is no sign of a broad anomaly in this temperature range but instead a maximum at lower temperatures ~6 K. In the original paper, this maximum was assigned to long-range antiferromagnetic order but without companion neutron diffraction or specific heat data, this cannot be confirmed. If the maximum is taken as a sign of short-range correlations, as in the case of the Re compound, then one can estimate a $J^{intra}/k \sim -4$ K for the Mo analog, more than 20 times smaller than the value of—89 K in the Re case. The origins of these remarkable differences in two isostructural materials are at yet unclear. One possibility is that the unpaired electrons reside in different, orthogonal π-orbitals in the two compounds. Electronic structure calculations would be helpful here.

Finally, it is worth mentioning again that no sign of long-range magnetic order can be detected in this material. The evidence is primarily negative, i.e., no divergence in the FC-ZFC susceptibility was noted down to 2 K. It is possible that any existing ordering is masked by the low-temperature paramagnetic tail. Further studies, especially those of the low-temperature heat capacity, should be carried out.

Acknowledgment

This work was financially supported by the Natural Sciences and Engineering Research Council of Canada through a Research Grant to J.E.G.

References

[1] M. Hase, I. Terasaki, K. Uchinokara, Phys. Rev. Lett. 70 (1993) 3651.
[2] R. Brusetti, B.K. Chakraverty, J. Devenyi, J. Dumas, J. Marcus, C.C. Schlenker, in: J.T. Devreese, L.F. Lemmens, V.E. Van Doren, J. Van Royen (Eds.), Recent Developments in Condensed Matter Physics, Plenum Press, New York, 1981.
[3] J.G. Bednorz, K.A. Muller, Z. Phys. B 64 (1986) 189.
[4] C. Kim, A.Y. Matsuara, Z.X. Shen, N. Motoyama, H. Eisaki, S. Uchida, T. Tohyama, S. Maekawa, Phys. Rev. Lett. 77 (1996) 4054.
[5] J.E. Greedan, N.P. Raju, A. Wegner, P. Gougeon, J. Padiou, J. Solid State Chem. 129 (1997) 320.
[6] R. Lam, F. Wiss, J.E. Greedan, J. Solid State Chem. 167 (2002) 182.
[7] W. Jeitschko, D.H. Heumannskamper, U.C. Rodewald, M.S. Schriewer-Pottgen, Z. Anorg, Allg. Chem. 626 (2000) 80.

[8] O. Muller, R. Roy, Mater. Res. Bull. 4 (1969) 349.
[9] A.D. Savel'eva, M.B. Varfolomeev, V.V. Fomichev, K.I. Petrov, Zh. Neorg. Khim. 22 (2994) (1977) 10.
[10] G. Baud, J.-P. Besse, M. Capestan, R. Chevalier, Ann. Chim. (Paris) 7 (1982) 615.
[11] G. Baud, J.-P. Besse, R. Chevalier, M. Gasperin, Mater. Chem. Phys. 8 (1983) 93.
[12] SAINT, release 4.05. Siemens Energy and Automation Inc., Madison, WI, 1996.
[13] G.M. Sheldrick, SADABS: Siemens Area Detector Absorption Correction Software, University of Göttingen, Germany, 1996.
[14] G.M. Sheldrick, Acta Crystallogr. A 46 (1990) 467.
[15] G.M. Sheldrick, SHELXL97, Program for the Refinement of Crystal Structures, University of Göttingen, Germany, 1997.
[16] N.L. Morrow, L. Katz, Acta Crystallogr. B 24 (1968) 1466.
[17] D.H. Heumannskämper, W. Jeitschko, Z. Kristallogr. 178 (1987) 99.
[18] K.A. Wilhelm, E. Lagervall, O. Muller, Acta Chem. Scand. 24 (1970) 3406.
[19] W. Jeitschko, D.H. Heumannskämper, M.S. Schriewer-Pöttgen, U.C. Rodewald, J. Solid State. Chem. 147 (1999) 218.
[20] A.S. Wills, VaList for GSAS, 1998.
[21] F.A. Cotton, Quart. Rev. (London) 20 (1966) 389.
[22] C.C. Torardi, C. Fecketter, W.H. McCarroll, F.J. DiSalvo, J. Solid State Chem. 60 (1985) 332.
[23] J.C. Bonner, M.E. Fisher, Phys. Rev. 135 (1964) 640.
[24] C.H. Weng, Ph.D. Dissertation, Carnegie Mellon University, 1968.
[25] W. Hiller, J. Strahle, A. Datz, M. Hanack, W.E. Hatfield, L.W. terHaar, P. Gutlich, J. Am. Chem. Soc. 106 (1984) 329.